Available online at www.sciencedirect.com
ScienceDirect
Procedia Engineering 10 (2011) 2214–2219
Engineering Procedia

ICM11

Martensitic transformation and texture in novel bcc Fe-Mn-Al-Ni-Cr alloys

E. P. Kwon[a,] *, S. Fujieda[a], K. Shinoda[a], S. Suzuki[a]

[a]*Institute of Multidisciplinary Research for Advanced Materials, Tohoku University, Katahira, Aoba-ku, Sendai 980-8577, Japan*

Abstract

Evolutions of martensitic transformation and texture during cold rolling in novel bcc Fe-Mn-Al-Ni-Cr alloys were studied. X-ray diffraction (XRD) and electron backscattering diffraction (EBSD) analyses revealed that this alloy undergoes α → ε → γ' martensitic transformation during deformation. At a 20% cold rolling strain, most of the α phase transformed into γ', and the transformed γ' phase had a Kurdjumov-Sachs (K-S) relationship with the parent α phase. Strong {*hkl*}<111> and weak {110}<001> transformation textures were formed after deformation. This texture evolution appeared to be related to the variant selection that occurred during the martensitic transformation.

Keywords: Fe-Mn-Al-Ni-Cr alloys; martensitic tranformation; texture; variant selection; EBSD

1. Introduction

Martensitic transformation in steels, particularly that induced by deformation, has numerous technological applications, e.g., in the production of advanced steels with high strength and good ductility [1] and introduction of the shape memory effect in alloys [2]. Thus far, most studies have shown that these types of steels undergo fcc γ to hcp ε phase and fcc γ to bcc (or bct) α' phase transformations during deformation. In general, bcc α to fcc γ' martensitic transformation is very rare. However, this transformation can occur in Fe-Mn-Al alloys prepared by suitable alloy design and heat treatment [3]. In this study, we carried out microstructural characterization of the martensitic transformation induced by deformation in novel bcc Fe-Mn-Al based alloys.

Although the martensitic transformation from the α phase to γ phase is rare, it has previously been reported to be occasionally observed in Fe-Mn-Al alloys quenched from high temperature [4-6]. These studies mainly dealt with the influence of carbon on the morphologies and structure of γ martensite formed by quenching from high temperature. Almost no study has reported deformation-induced α to γ' martensitic transformation in Fe-Mn-Al alloys. However, in a very recent study [3], Ando et al. observed this unique α → γ' martensitic transformation by cold rolling Fe-Mn-Al-based alloys at room temperature. They found that at a 50% cold rolling strain, the α phase was completely transformed to γ' martensite, and the transformation process was accompanied by a magnetic transition from a ferromagnetic state to a weakly magnetic state. They attributed this unique phase change to the formation of the abnormal shape of the α/γ phase equilibrium due to the magnetic effect of the alloy with a specific

* Corresponding author. Tel.: +81-(0)22-217-5177
E-mail address: ackep@mail.tagen.tohoku.ac.jp

Selection and peer-review under responsibility of ICM11 doi:10.1016/j.proeng.2011.04.366

composition. This implies that a change in the composition of this Fe-Mn-Al system might have a significant effect on the martensitic transformation because both the magnetic properties and the α/γ phase equilibrium are influenced by the composition. Although they have investigated the origin of the martensitic transformation and the structure of the γ' martensite in the Fe-Mn-Al alloys, the microstructural and crystallographic aspects related to this transformation have not yet been investigated in detail. In this paper, we report on the martensitic transformation behavior, crystallographic orientation relationship (OR) between the parent phase and transformed phases, and the transformation texture in cold-rolled novel bcc Fe-Mn-Al-Ni-Cr alloys.

2. Experimental procedures

Fe-35Mn-15Al-7Ni-2Cr alloy sheets (mass%) were prepared by induction melting and hot rolling. Small samples for mechanical tests were solution heat treated at 1200 °C for 30 min under vacuum and then quenched in water to obtain α single phase. Fully ferritic (bcc) phase was obtained when samples were dipped into water within 3 seconds while martenstie (fcc) phase were formed together with the ferrite phase when the time was about 5 seconds. Microstructural features of samples deformed by cold rolling were studied using electron backscattering diffraction (EBSD). EBSD patterns were obtained using a Nordlys II EBSD detector mounted on a Hitachi SU-6600 FE-SEM operating at an acceleration voltage of 15 kV. EBSD data were post-processed by HKL CHANNEL 5 flamenco software to obtain microstructural information. Since the detection ratio for martensite phases was low, data clean-up using the EBSD software was carried out before the EBSD post-processing. Texture analysis was carried out using the EBSD orientation distribution function (ODF) and the inverse pole figure. In the texture analysis, to obtain reliable statistical results, an EBSD map stitched from six individual maps by using a HKL map stitcher was used. X-ray diffraction (XRD) measurements were performed using a Rigaku RINT-2200 diffractometer with Mo Kα radiation. Prior to microstructural analysis, all samples were electropolished in a solution of 20 vol% perchloric acid in acetic acid to eliminate traces of machining as well as to remove the oxide layer formed on the sample surface during heat treatment.

3. Results and discussion

3.1 XRD analysis of cold rolled samples

Martensitic transformation occurring during cold rolling was first analyzed by XRD. XRD patterns of as-quenched and cold-rolled samples are shown in Fig. 1. The results indicate that the as-quenched sample is fully ferritic. With increase in the strain to 5% and then to 20%, the intensities of ferrite main peaks are reduced, but simultaneously, several γ' martensite peaks appear. Interestingly, at the intermediate deformation stage of 5% strain, an ε martensite peak is observed. These results imply that the ε phase as well as the γ' phase are induced by a rolling deformation of 5% strain, and they coexist with the remaining α phase in the deformed microstructure. At a higher strain of 20%, most of the α phase transforms into γ' martensite and the ε peak is no longer present in the XRD pattern. The abovementioned measurements were conducted with the same sample and at approximately the same position in order to directly compare the martensitic transformation behavior at each stage of deformation. Obviously, the presence of the ε martensite peak at only the 5% strain level implies that this alloy undergoes α → ε → γ' martensitic transformation.

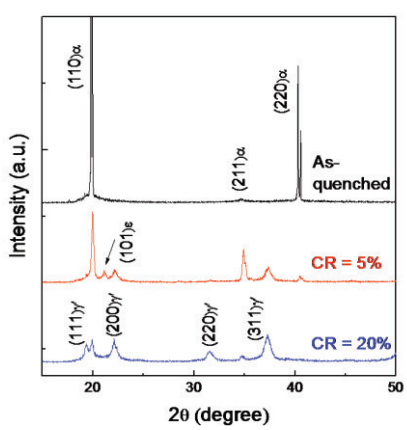

Fig. 1 XRD patterns of as-quenched and cold-rolled (5% and 20% accumulated strains) Fe-Mn-Al-Ni-Cr alloy. The XRD patterns were measured with Mo Kα radiation.

3.2 Orientation relationship between parent α and transformed ε and γ' phases

Since this Fe-Mn-Al-Ni-Cr alloy undergoes martensitic transformation under deformation, the parent and daughter phases are expected to have some crystallographic OR. To investigate this OR, the γ' and ε martensite plates in a selected α grain were chosen, and their representative pole figures were obtained (Fig. 2). After comparing the coincident poles in the pole figures, the ORs between these three phases were determined to be {110}α//{111}γ'//{0001}ε and <111>α//<110>γ'//<1120>ε. The OR between α and γ', therefore, corresponds to the Kurdjumov-Sachs (K-S) relationship. Each pole shows slight deviation from this orientation correspondence. This deviation may be responsible for the grain distortion and lattice rotation induced during plastic deformation and for the limited angular resolution of EBSD. This relationship has also been found in some stainless steels and ferrous shape memory alloys, which undergo a two stage γ → ε → α' transformation [7,8]. The result of OR analysis along with the result of XRD analysis suggests the occurrence of some special phenomena in this novel Fe-Mn-Al-Ni-Cr alloy: α → γ' transformation occurring due to deformation is accompanied by an intermediate deformation stage of α → ε. That is, the martensitic transformation process in this alloy is expressed by a two stage α → ε → γ' transformation. The suggested α → ε → γ' transformation process is simply the reverse of the abovementioned γ → ε → α' process, and it proceeds with the same OR that is found in the γ → ε → α' process. As observed, the parent α phase and the transformed γ' phase have a K-S relationship. Theoretically as there are 24 possible K-S variants, unless variant selection occurs, the α → γ' transformation must result in 24 different variants in a single α grain. However, in the alloy under study, this was never achieved when γ' martensite was induced by deformation. As observed in Fig. 2 and as will be seen in Fig. 3, only a limited number of variants are formed within a deformed α grain.

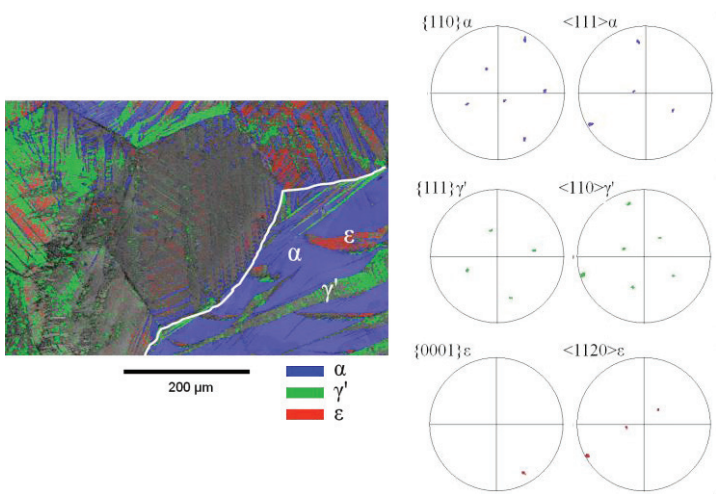

Fig. 2 EBSD phase map for several grains of 10% cold-rolled Fe-Mn-Al-Ni-Cr alloy (left), and experimental pole figures for three phases *i.e.*, α, γ', and ε obtained in a single α grain (right).

3.3 γ' martensite variants

To observe the formation and growth of γ' martensite variants during cold rolling, the deformed microstructure was measured by EBSD. By using an Euler map, it was possible to easily detect individual variants that developed in the microstructure. Figure 3 shows that the microstructure of the as-quenched sample consists of equiaxed α grains. Thin lines and plates are observed in the microstructure of the 5% cold-rolled sample, which correspond to γ' phases. In the selected α grain, only three distinct γ' martensite variants—denoted as M1, M2, and M3—are observed. M1 and M3 are paired, but they can be clearly distinguished in the Euler map by their different Euler angles, i.e., M1: (15°, 20°, and 62°) and M3: (320°, 10°, and 22°). With further deformation corresponding to a 20% strain, only M2 was found to be formed predominantly within the α grain. This strong variant selection may induce strong transformation texture, which will be discussed subsequently. In Fig. 3 (c), some pixels corresponding to M3 were detected in a slightly different area from that observed in Fig. 3 (b). This was because about 1–2 μm of the

sample surface was removed by electrochemical polishing after the final rolling step so as to eliminate the contaminated area and surface relief caused by the shear transformation, with the aim of improving the efficiency of the EBSD detector. Despite this treatment, the transformed martensite phases have relatively lower image pattern quality and lower band contrast value (Fig. 3 (d)) than the parent α phase. The low image contrast observed for the martensite phases can be possibly related to their high defect density, which would result in their poor Kikuchi pattern quality. According to the results of the transmission election microscopy (TEM) study by Ando et al. [1], γ' martensite, which possesses an fcc crystal structure, contains a high density of crystalline defects, e.g., twins.

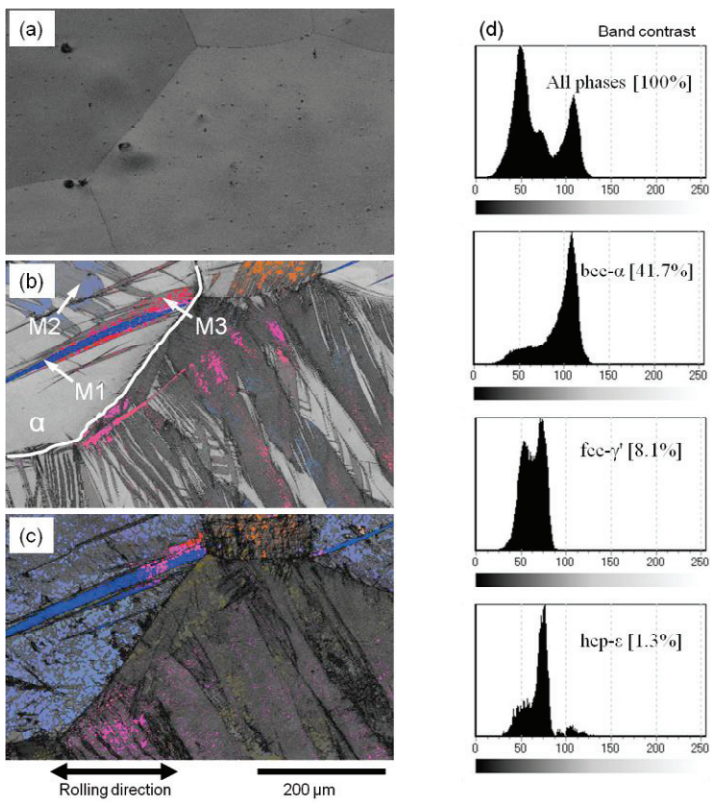

Fig. 3 EBSD band contrast maps with Euler maps for fcc phase; (a) as-quenched, (b) 5% strain, and (c) 20% accumulated strain. (d) Band contrast graphs obtained from Fig. 3 (b). M1, M2, and M3 denote different variants.

γ' martensite can also be formed by water quenching. Fig. 4 (a) shows that the morphology of the martensite plates is different from those induced by deformation. However, it was found that they also have an OR with the parent α phase. The theoretical {110} pole figure (Fig. 4 (b)) of the K-S relationship variants is comparable to that of the experimental {110}γ' pole figure (Fig. 4 (c)). (Here, we presented only raw data without rotation simulation.) From the experimental {110}γ' pole figure, it was confirmed that γ' martensite has a K-S relationship with the α phase and that almost all the 24 K-S variants were well developed. The contoured pole figure in Fig. 4 (d) shows that the variants located near the center pole (marked by an arrow) have a very high contour intensity level compared to other variants. This result indicates that although all the 24 K-S variants are formed during water quenching, at least one martensite variant is formed more selectively.

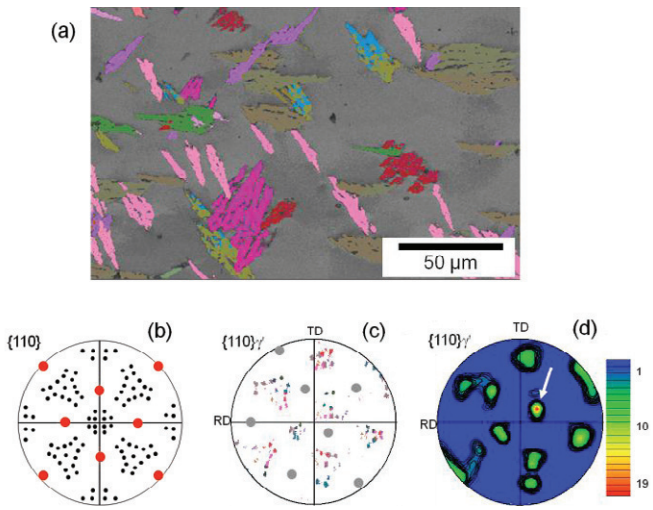

Fig. 4 (a) Euler map showing γ' martensite plates formed by water quenching in Fe-Mn-Al-Ni-Cr alloy. (b) Theoretical {110} pole figure of K-S martensite variants. The red dots represent the {110} poles of the parent phase. (c) Experimental {110}γ' pole figure obtained from single α grain and (d) corresponding contoured pole figure.

3.3 Texture evolution by cold rolling and quenching

A comparison between the textures of the γ' martensite in the deformed and water-quenched alloys is shown in Fig. 5. Here, the term "water-quenched" is used to differentiate it from the previously used term "as-quenched." Visual inspection of the ODF shows that the textures developed in the deformed and water-quenched alloys are similar. The ODF in Fig. 5 (a) shows that the deformed alloy has two main texture components that can be indexed to a strong {*hkl*}<111> and a weak Goss texture {110}<001>. The evolution of this strong {*hkl*}<111> texture may be related to this observed intense variant selection. In the case of the water-quenched sample, weaker {*hkl*}<111> and stronger {110}<001> textures are found. It is worthwhile to note that in the ODF in Fig. 5 (b), there is very large scatter from ideal textures and even some scattered region cannot be identified as having any texture. This large scatter in the water-quenched alloy can be attributed to the less intense variant selection (Fig. (4)), which can result in the spread of orientation distribution owing to the formation of different variants. In several materials, variant selection is apparently correlated to the formation of texture [9,10]. In this alloy, when martensitic transformation occurred by deformation, the number of selected variants in the α grain was found to be much lower than the theoretically allowed 24 K-S variants. In that case, the alloy exhibited a strong transformation texture of {*hkl*}<111>.

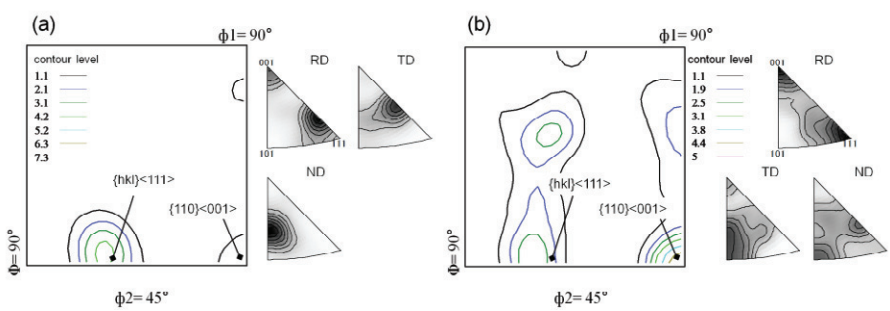

Fig. 5 Textures of γ' martensite formed by (a) cold rolling under 20% strain and (b) water quenching in Fe-Mn-Al-Ni-Cr alloy. ODF is ϕ2 = 45° section.

4. Conclusions

Martensitic transformation and texture evolution in cold-rolled Fe-Mn-Al-Ni-Cr alloys were investigated through XRD and EBSD analyses. At 20% cold rolling, most of the α phase was found to be transformed into γ' martensite. At an intermediate rolling strain of 5% and 10%, ε martensite coexisted with α and γ'. This result indicates that the α → γ' transformation is a two-step process resulting from stepwise α → ε and ε → γ' transformations. The ORs among the α, ε, and γ' phases were found to be {110}α//{0001}ε//{111}γ' and <111>α//<1120>ε//<110>γ', which indicated that the parent α phase had a K-S relationship with the transformed γ' martensite. The γ' martensite formed in water-quenched alloys showed a weak {*hkl*}<111> texture with large scatter, which may be responsible for the formation of all the 24 K-S variants. On the other hand, not all of the 24 γ' variants developed with equal frequency during cold rolling. Instead, specific variants were formed favorably, thereby contributing to the development of the observed strong {*hkl*}<111> transformation texture.

Acknowledgements

This work was supported by the Global COE Program "Materials Integration (International Center of Education and Research), Tohoku University, of MEXT, Japan.

References

[1] B. C. De Cooman, Curr. Opin. Solid State Mater. Sci. 2004;**8**:285-303.

[2] A. Sato, E. Chishima, K. Soma, T. Mori, Acta Metall. 1982;**30**:1177-1183.

[3] K. Ando, T. Omori, I. Ohnuma, R. Kainuma, K. Ishida, Appl. Phys. Lett. 2009;**95**:212504.

[4] K. H. Hwang, C. M. Wan, J. G. Byrne, Scr. Metall. Mater. 1990;**24**:979-984.

[5] W. S. Yang, K. H. Hwang, T. B. Wu, J. G. Byrne, C. M. Wan, Scr. Metall. Mater. 1990;**24**:1221-1224.

[6] W. C. Cheng, C. F. Liu, Y. F. Lai, Scr. Mater. 2003;**48**:295-300.

[7] M. Humbert, B. Petit, B. Bolle, N. Gey, Mater. Sci. Eng. A 2007;**454-455**:508-517.

[8] K. Shimizu, Y. Tanaka, Trans. JIM 1978;**19**:685-693.

[9] M. R. Daymond, R. A. Holt, S. Cai, P. Mosbrucker, S. C. Vogel, Acta Mater. 2010;**58**:4053-4066.

[10] S. H. Lee, J. Y. Kang, H. N. Han, K. H. Oh, H. C. Lee, D. W. Suh, S. J. Kim, ISIJ Int. 2005;**45**:1217-1219.